Environ Sci Pollut Res (2016) 23:18911–18927
DOI 10.1007/s11356-016-7077-3

RESEARCH ARTICLE

Hydrogeochemical features of surface water and groundwater contaminated with acid mine drainage (AMD) in coal mining areas: a case study in southern Brazil

Juliana Aparecida Galhardi[1] · **Daniel Marcos Bonotto**[1]

Received: 18 January 2016 / Accepted: 13 June 2016 / Published online: 22 June 2016

Abstract Effects of acid mine drainage (AMD) were investigated in surface waters (Laranjinha River and Ribeirão das Pedras stream) and groundwaters from a coal mining area sampled in two different seasons at Figueira city, Paraná State, Brazil. The spatial data distribution indicated that the acid effluents favor the chemical elements leaching and transport from the tailings pile into the superficial water bodies or aquifers, modifying their quality. The acid groundwaters in both sampling periods (dry: pH 2.94–6.04; rainy: pH 3.25–6.63) were probably due to the AMD generation and infiltration, after the oxidation of sulfide minerals. Such acid effluents cause an increase of the solubilization rate of metals, mainly iron and aluminum, contributing to both groundwater and surface water contamination. Sulfate in high levels is a result of waters' pollution due to AMD. In some cases, high sulfate and low iron contents, associated with less acidic pH values, could indicate that AMD, previously generated, is nowadays being neutralized. The chemistry of the waters affected by AMD is controlled by the pH, sulfide minerals' oxidation, oxygen, iron content, and microbial activity. It is also influenced by seasonal variations that allow the occurrence of dissolution processes and the concentration of some chemical elements. Under the perspective of the waters' quality evaluation, the parameters such as conductivity, dissolved sodium, and sulfate concentrations acted as AMD indicators of groundwaters and surface waters affected by acid effluents.

Keywords Coal mine · Acid mine drainage · Groundwater contamination · Sulfate · Iron · Water quality indicator

Responsible editor: Philippe Garrigues

✉ Juliana Aparecida Galhardi
julianagalhardi@yahoo.com.br

[1] Departamento de Petrologia e Metalogenia, Instituto de Geociências e Ciências Exatas, Universidade Estadual Paulista "Júlio de Mesquita Filho", Campus de Rio Claro. Avenida 24-A, No. 1515, CP 178, Rio Claro, São Paulo 13506-900, Brazil

Introduction

Coal mining and mineral processing generates large volumes of waste rock and mill tailings, corresponding to the main sources of environmental impacts related to mining activities as the oxidation of sulfide minerals present in these materials can result in acid mine drainage (AMD) generation (Fungaro and Izidoro 2006).

This acid effluent is characterized by high concentrations of sulfate, iron (from sulfide minerals oxidation), aluminum (from weathering of the host rocks), and trace elements (Blowes et al. 2014; Carrero et al. 2015; Qureshi et al. 2016), representing a recalcitrant environmental problem. It affects active and abandoned mining areas around the world (Younger et al. 2002; Carrero et al. 2015) where the leaching and dispersion of the toxic metals cause environmental damage to both surface and groundwaters, until complete weathering of pyrite and other sulfide minerals (Nordstrom 2009). The AMD flow into groundwater, streams, and rivers gives rise to several environmental problems. Despite neutralization of the acidity, the AMD can still affect humans and wildlife indirectly, for instance, by sedimenting toxic metals in fluvial systems (Simate and Ndlovu 2014).

The acid effluent is produced when sulfide minerals are exposed to oxygen and water, promoting a sequence of reactions that lead to pH reduction (generally below 3) and release of metals, such as iron and aluminum. Pyrite is the main mineral responsible for AMD generation. When pyrite surfaces

are exposed to water and an oxidant (including O_2 and Fe(III)), the mineral oxidation occurs through chemical, biological, or electrochemical pathways, in oxic or anoxic systems (Nordstrom et al. 2015).

AMD is known by its toxicity to aquatic organisms but it can contain an abundant microbial life responsible for catalyzing the generation of acid effluents (Francis 1990). Two major bacterial species involved in this process are *Acidithiobacilus thiooxidans* and *Acidithiobacilus ferroxidans*, which oxidize sulfur and iron, respectively (Francis 1990; Silva et al. 2011). In their absence, pyrite is not expressively oxidized and Fe(III) is not produced at a significant rate. The following reactions represent the AMD generation (Al-Hashimi et al. 1996; Akcil and Koldas 2006):

$$FeS_2 + {}^{7}/_{2}O_2 + H_2O \rightarrow Fe^{2+} + 2SO_4^{2-} + 2H^+ \quad (1)$$

$$Fe^{2+} + {}^{5}/_{2}H_2O + {}^{1}/_{2}O_2 \rightarrow Fe(OH)_3\downarrow + 2H^+ \quad (2)$$

$$Fe^{2+} + {}^{1}/_{4}O_2 + H^+ \rightarrow Fe^{3+} + {}^{1}/_{2}H_2O \quad (3)$$

$$FeS_2 + 14\,Fe^{3+} + 8\,H_2O \rightarrow 15\,Fe^{2+} + 2\,SO_4^{2-} + 16\,H^+ \quad (4)$$

Pyrite is oxidized by oxygen, sulfur turns to sulfate (SO_4^{2-}) and ferrous iron (Fe(II)) is released (Eq. 1), giving rise to two moles of acidity (H^+) for each mole of oxidized pyrite. Iron and other metals can react with alkali compounds (e.g., naturally occurring calcite and dolomite, depending on the geologic characteristics close to the coal horizons, or calcareous material added in the rejects dump to the pH control) resulting in insoluble (hydr)oxides, or precipitates, in solution (Eq. 2). Once the alkalinity available is depleted, metals can return to solution. The Fe(III) concentration increases (Eq. 3), acting as an oxidizing agent to pyrite (Lottermoser 2010) (Eq. 4), characterizing a cyclical process that occurs until the ferric iron or pyrite becomes exhausted. The final product is iron in soluble (Fe(II)) or solid ($Fe(OH)_3$) forms. At low pH conditions, the ferric iron solubility increases, as well as its availability as an oxidizing agent. It is also influenced by the Eh, the buffering capacity and dissolved organic matter content in solution (Küsel 2003).

During the AMD generation, water is a reagent, a medium for bacteria in the oxidation process and a transport way for the oxidation products (USEPA 1994; Geldenhuis and Bell 1998). An amount of atmospheric oxygen is also required for the oxidation of sulfide minerals, in order to ensure the catalyzation of the process by bacteria (Berghorn and Hunzeker 2001). In areas below the water table, oxygen diffusion is slow and minor acids will be produced, differently from areas above it where there is a contact between the sulfide minerals, atmospheric oxygen, and water (Berghorn and Hunzeker 2001). Thus, iron is usually found as Fe(II) where limited oxygen is present, but it is found as Fe(III) in atmospheric conditions where oxygen and microbiological activities are abundant (Nordstrom and Alpers 1999; Silva et al. 2013).

Seasonal variations can also affect the acid production (USEPA 1994) and rainfall events can cause both increases and decreases in the AMD generation and leaching of the metals (Nordstrom 2009). The rainwater infiltration into the reject dump promotes metal leaching and the water contamination. Simultaneously, dilution of metals and compounds occurs, as rainwater increases the water volume into the stream, improving the water quality (Lee et al. 2001).

Caraballo et al. (2016) proposed three hydrochemical stages for AMD in a sulfide mining district: a high metal concentration with a low flow rate; an extreme metal concentration with a high flow rate; a mixed situation comprising a high flow rate, and medium high metal concentration. In addition to seasonal variations, important processes controlling the spatial distribution and concentration of elements in streams affected by AMD are dilution by mixing, co-precipitation/adsorption, redox processes, and pH fluctuations (Shim et al. 2015). In aquifers, the AMD extension can be controlled by advection through the fractures, diffusion-controlled transport into the porous matrix, diffusion from the matrix into the fractures, pH buffering by carbonate, and silicate minerals as well as loss of sulfate and iron due to gypsum and ferrihydrite precipitation (Molson et al. 2012).

The acid effluents may or may not contain dissolved toxic metals, but will always contain sulfate in their composition (Wolkersdorfer 2008). Effluents with high sulfate and low dissolved iron content can be indicative of the previously generated AMD, that is being neutralized nowadays (Berghorn and Hunzeker 2001). Similarly, as the AMD generation consumes 1 mol of acidity (Eq. 3) and culminates in iron oxidation, if the effluent contains abundant dissolved ferrous iron, it may indicate that chemical reactions are in the middle way in the pyrite oxidation process, i.e., some iron was not oxidized according to Eq. 3.

Sulfate and electrical conductivity (EC) have been used as monitors of the AMD occurrence in natural waters, since iron and other metals are unstable in solution (USEPA 1994; Gray 1996). Sulfate is a conservative compound, naturally present in surface and groundwaters and its background concentration in waters is usually low, different from areas whereby coal mining takes place. Iron, aluminum, and other metals may not remain in solution in AMD, but SO_4^{2-} is very soluble, chemically stable, and not removed in a significant proportion by physico-chemical processes during the wastewater treatment. Gray (1996) used regression analysis for avoiding technical problems related to SO_4^{2-} measurements in field and proposed use of the EC to predict the SO_4^{2-} concentration in both AMD and contaminated surface waters because EC is

very sensitive to SO_4^{2-} ions and both are characterized in AMD even under condition of large dilution in the water body.

The safety assessment of a waste deposit containing toxic elements should predict their migration into natural waters (Baik et al. 2003) that is an important transport route for the pollutants. Accurate prediction of AMD is required in order to determine how to bring the acid effluent under control (Geldenhuis and Bell 1998). The AMD hydrochemistry is expected to be significantly influenced by seasonal fluctuations and only few researches have been developed in tropical areas of southern hemisphere. In this context, this paper evaluates how the AMD affects the quality of the natural waters in a coal mining area at Figueira city, Paraná State, Brazil, and proposes some chemical indicators for groundwaters and surface waters affected by acid effluents.

Study area

Coal is the largest source of non-renewable fuel to electricity generation in Brazil and the largest reserves are situated in the states of Rio Grande do Sul, Santa Catarina, Paraná and São Paulo, respectively. The coal mining area studied in this paper is located at Figueira city, in the northern part of Paraná State (Fig. 1). The region is within the hydrographic sub-basin of Cinzas River, the main watercourse in the northern part of Paraná State, whose main tributaries are Grande, Jaboticabal and Vermelho streams and Laranjinha (Peixe) River (SEMA 2010). The last one discharges into the Paranapanema River.

The climate in the area is humid subtropical, with rains during October to March and dry from April to September. January is the month with the highest rainfall (~245 mm), while the lowest rainfall occurs in August (~45 mm) (Fig. 2).

The study area is situated in the Paraná Sedimentary Basin that spreads in Paraná, Mato Grosso, Mato Grosso do Sul, Goiás, São Paulo, Santa Catarina, and Rio Grande do Sul states in Brazil, as well as in other countries like Uruguay, Argentina, and Paraguay. In the region, the outcropping stratigraphic units are of Permian age, belonging to Itararé Group, Guatá Subgroup (Rio Bonito and Palermo formations), and Passa Dois Group (Irati, Sierra Alta, and Teresina formations) (Shuqair 2002; Bizzi et al. 2003).

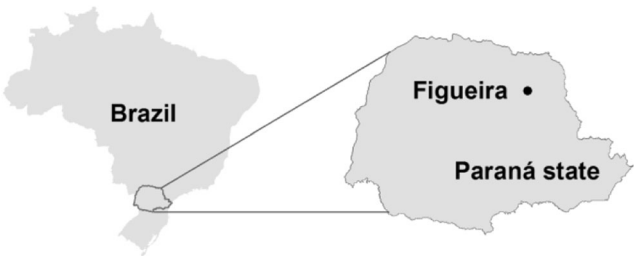

Fig. 1 Location of the study area

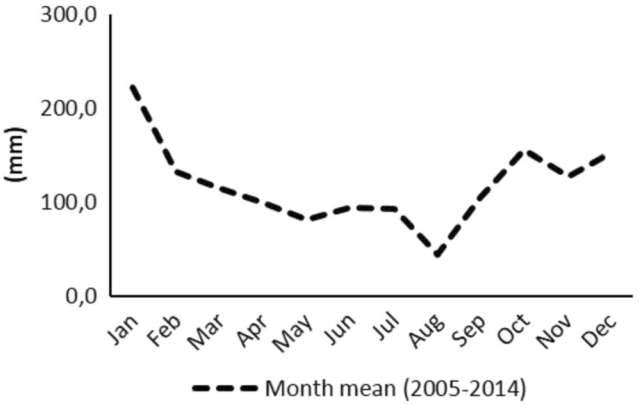

Fig. 2 Monthly precipitation from 2005 to 2014 in Figueira city, Paraná State, Brazil

The coal horizons are restrained in Rio Bonito Formation that is 120–140 m thick and is covered by Itararé Group. This formation comprises of three members in the eastern portion of the Paraná basin (Schneider et al. 1974): Triunfo (composed by fine to medium and thick sandstones, also occurring siltstones and coal layers); Paraguaçu (composed by siltstones and bioturbed shales combined with fine sandstone and carbonate rocks); and Siderópolis (composed by thin sandstones interspersed with carbonaceous shales and coal).

The coal deposit in the study area (estimated to be 22.7 Mt) is part of the largest coal reserve still in exploitation in Paraná State (Bizzi et al. 2003). It is composed of plant debris that was reworked and concentrated by marine agents (Zacharias and Assine 2005). The coal horizons are 0.50–0.65 m thick, occurring at a variable depth of 38–75 m (ANEEL 2011). In this area, the coal exhibits high sulfur content (7 to 12 %) (MINEROPAR 2001; ANEEL 2011) that may influence the AMD generation rate. The coal mining is an economic activity of great importance to the local community, employing directly and indirectly hundreds of people since the 1950s. In 1959, a thermal power plant started operating in the Figueira city.

The coal exploration has taken place in open and underground pit and nowadays just one underground mine is operating. Environmental impacts of complex recovery have been identified due to decades of coal mining activities. For example, vegetation has been removed from the site, relief has undergone drastic changes, and the groundwater table is now at the terrain surface. Modification on the chemical composition of surface waters and bottom sediments has been also verified, for instance, pH lowering and increase of Al^{3+}, Ca^{2+}, Sr^{2+}, Mn^{2+}, Na^{+}, SO_4^{2-}, and $Cd_{(total)}$ concentrations close to the coal mine relatively to other areas in Paraná State (Licht 2001).

The water used for coal washing after its crushing has been recycled in a closed system and physically treated in a pond. This pond also receives the acid effluent generated in the tailings. Eventually, the effluents may reach the soil, groundwater and surface water, modifying their chemical

composition and contributing to the water contamination. The rejects have been disposed in two main tailings pile. The first (older than 50 years) is not waterproofed, operating without carbonate addition to the pH control. The second has accumulated materials with high pyrite concentration, has been waterproofed and operating with the CaO addition. The tailing piles are located in an outcrop area of Palermo Formation that is composed by clays and siltstones interlayered with sandy layers (Krebs and Alexandre 1998). It is a convenient groundwater reservoir as its basal portion comprises sandy material.

Campaner and Luiz-Silva (2009) and Campaner et al. (2014) investigated the AMD effects on soils, surface waters, and groundwaters from the Figueira city, checking the effluent quality after a treatment to the pH control by CaO addition. They found a pH increase in the surface waters downstream the mine that was attributed to carbonate minerals present in soils/rocks of the area and also to the CaO added in the tailings pile. Another finding was the increase in the toxic metals in the waters close to the mine (Campaner and Luiz-Silva 2009; Campaner et al. 2014).

Material and methods

Groundwaters, surface waters, and effluents were sampled in the coal mining area in August 2013 (dry season; monthly rainfall = 1.1 mm) and February 2014 (wet season; monthly rainfall = 341.6 mm). The rainfall data (Fig. 2) suggests that the water discharge was greater in February 2014 than in August 2013, although it was not determined in the surface water sampling points: Laranjinha River (main water course in the region) and Pedras stream, its affluent. The bores for the groundwater monitoring were located within the mining area and its upstream.

Samples identified as P1–P8 refer to groundwater, E1 refers to effluents sampled in drainage pipes from the reject dump with no environmental control (without CaO addition) and E2 corresponds to effluents sampled directly in the reject dump where CaO is mixed with the rejects and there is waterproofing for avoiding water infiltration. Samples identified as L1 and L2 refer to Laranjinha River, respectively, upstream and downstream the mine. RP1 and RP2 refer to water sample from Pedras stream, respectively, upstream and downstream the mine, as indicated in Fig. 3.

The groundwaters were sampled using a bailer whereas the surface waters and effluent samples were taken using a manual collector. The samples were stored in 1-L polyethylene flasks and the dissolved oxygen (DO) concentration was measured in situ using a portable detector (Hanna/HI 9146), as well as temperature, pH (Digimed/DM-2P) and EC (Hanna/HI 9146). The redox potential (Eh) was measured with an Analion/IA601 meter that was connected to a combined Pt electrode (Analion/674) and was calibrated using a Zobell solution, as described by Bonotto (1996). All the devices were properly calibrated before the field works.

The chemical analyses were performed at LABIDRO - Isotopes and Hydrochemistry Laboratory, UNESP, Rio Claro, São Paulo, Brazil. The samples were filtered by 0.45-μm porosity and 47-mm diameter Millipore membrane, the suspended solids (SS) were determined by gravimetry, bicarbonate by titration and the major chemical parameters (phosphate, sulfate, chloride, nitrate, silica, barium, calcium, magnesium, ferric iron, total iron, and potassium) were determined by colorimetry that was performed with the portable Hach-DR/2000 spectrophotometer. Ferrous iron was determined from total iron and ferric iron values given by the Hach-DR/2000 spectrophotometer.

Sodium was determined by inductively coupled plasma optical emission spectrometry (ICP-OES) in the Center for Environmental Studies (CEA - UNESP, Rio Claro, São Paulo, Brazil). Organic matter was quantified by the chemical oxygen demand (COD, in mg $O_2.L^{-1}$) method that indicates the oxidant amount required to the organic matter oxidation. The technique uses a strong oxidizing agent ($K_2Cr_2O_7$) and a catalyst (Ag_2SO_4) in an acidic medium, used to convert the organic matter into carbon dioxide and water. After the oxidation process, the COD concentration was obtained by colorimetry (Hach-DR/2000 spectrophotometer). All the data of the measured parameters is given in Tables 1, 2, and 3 (August 2013) and in Tables 4, 5, and 6 (February 2014).

Results and discussion

Water quality and effluent discharge

In Brazil, the standards for water quality are described in CONAMA Resolution No. 357 (CONAMA 2005), which classifies the surface waters by biological, chemical, and physico-chemical parameters and also according to the intended use for each water body. According to this resolution, Laranjinha River and Pedras stream are classified into class II that comprises the following uses of the water bodies: human consumption after simplified treatment, protection of aquatic communities, recreation activities, aquaculture, and irrigation.

The CONAMA resolution no. 430 (CONAMA 2011) regulates the waste water discharge into natural water bodies and establishes conditions and standards for the effluents discharge into the surface waters according to its classification, i.e., the effluents must exhibit pH between 5 and 9 and should not contain dissolved iron concentration above 15 mg L^{-1}, if they are released into class II waters. The samples E1 and E2 exhibited values for these parameters not fitting these guidelines. In the past, the effluents generated in the tailings were

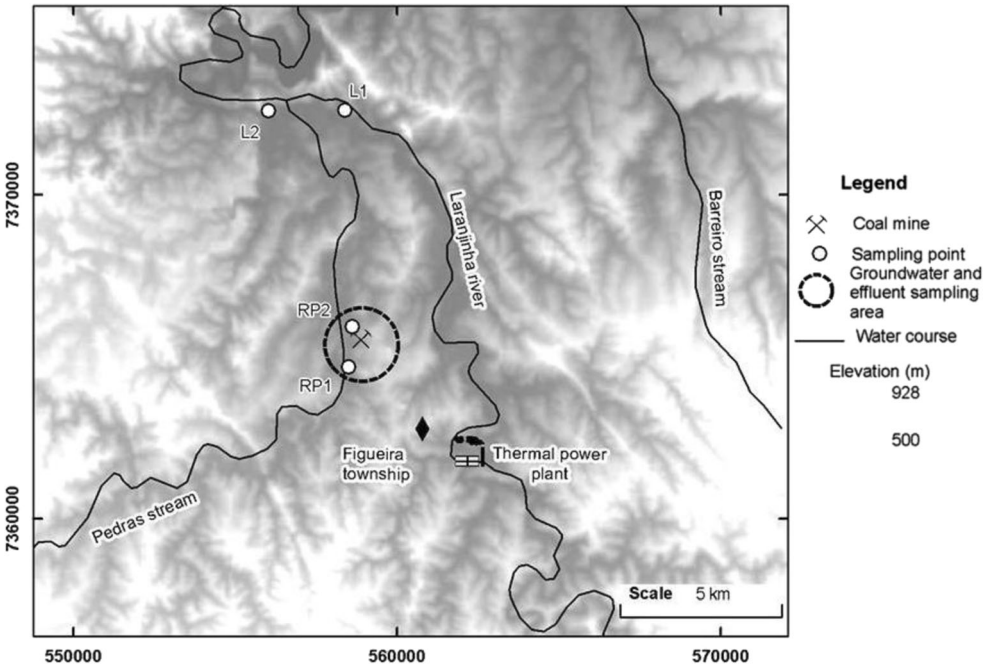

Fig. 3 Location of the sampling points

directly discharged into Pedras and Mina streams, but nowadays they receive a physico-chemical treatment in a sedimentation pond with the addition of carbonate materials to remove the particulate matter and to allow the metal precipitation before returning to the coal processing in a closed system. A portion of this effluent can reach the local soil and be transported to the streams.

Aluminum, barium, and total iron in the surface waters exhibited values higher than the permitted limits by the CONAMA standards (CONAMA 2005) in some samples. For instance: aluminum (maximum allowed is 0.1 mg L^{-1})—exceeded in RP2 and L1 samples (dry season); barium (maximum allowed is 0.7 mg L^{-1})—exceeded in L1, L2, RP1, and RP2 samples in both monitoring periods; total iron (maximum allowed is 0.3 mg L^{-1})—exceeded in L1 and L2 samples (dry season) and in RP1, L1, and L2 samples (wet season).

The increase in the concentrations of some compounds in the groundwaters is affected by the AMD. The extremely high sulfate and iron concentrations modify the chemical equilibrium of the waters, as verified in some groundwater samples (both periods).

Table 1 Physico-chemical parameters for waters and effluents samples collected in August/2013

Sample	Temperature (°C)	pH	DO (mg L^{-1})	COD (mg L^{-1})	Conductivity (mS cm^{-1})	SS (mg L^{-1})	Eh (mV)
P1	20.5	5.34	7.34	21.12	0.02	63.0	285
P2	20.7	3.71	6.25	40.48	0.53	3239.0	437
P3	20.7	3.80	6.55	59.84	1.28	17.5	420
P4	21.5	2.94	6.29	15.84	3.32	993.0	355
P5	20.3	3.21	6.33	40.48	1.25	431.0	460
P6	22.5	4.03	6.75	N.M.	1.82	1364.0	462
P7	21.2	3.72	6.72	26.40	2.56	53.4	496
P8	24.9	6.04	1.30	29.92	4.26	373.0	330
RP1	16.5	7.26	7.47	1.76	0.10	2.0	318
RP2	17.1	6.95	7.56	1.76	0.17	12.0	212
L1	18.5	7.04	7.69	3.52	0.05	19.0	228
L2	17.3	6.88	7.48	14.08	0.07	86.0	342
E1	26.1	6.24	5.80	1.76	2.08	292.0	468
E2	27.8	4.01	6.26	14.08	3.10	259.0	376

N.M. not measured

Table 2 Major cations in waters and effluents samples collected in August 2013

Sample	Sodium (mg L^{-1})	Potassium (mg L^{-1})	Calcium (mg L^{-1})	Magnesium (mg L^{-1})	Ferrous iron (mg L^{-1})	Ferric iron (mg L^{-1})	Barium (mg L^{-1})	Aluminum (mg L^{-1})	Silica (mg L^{-1})
P1	4.39	0.80	11.28	2.00	0.01	3.00	1.5	1.30	19.6
P2	127.00	11.70	8.00	4.32	4.20	6.10	4.5	2080.00	15.5
P3	17.50	0.74	2.00	0.38	18.00	566.00	52.5	1067.00	105.6
P4	54.60	10.00	1.00	5.00	22.40	988.00	285.0	2542.00	N.M.
P5	22.80	41.00	26.16	2.00	3.50	131.00	117.0	44.85	0.7
P6	35.22	2.32	1.00	1.42	1.84	20.30	4.0	1090.00	21.3
P7	103.00	16.10	33.20	2.00	0.01	1.45	3.0	4.00	18.3
P8	859.00	49.70	196.00	1400.00	0.05	2.75	45.0	1.30	1.7
RP1	5.10	2.66	2.00	3.04	0.01	0.14	4.7	0.96	14.6
RP2	9.74	2.70	2.00	3.28	0.01	0.01	3.0	1.30	17.6
L1	3.07	2.24	1.00	0.24	0.01	0.30	2.0	12.50	12.7
L2	3.21	2.26	10.00	4.60	0.00	0.35	1.5	0.07	11.9
E1	144.00	26.00	1.00	1.36	0.02	21.98	5.0	1.00	11.9
E2	96.10	28.50	38.00	1.00	26.00	2824.00	120.0	1317.50	N.M.

N.M. not measured

Effects of the rainfall on the overall chemical composition of the waters

The Piper (1944) diagram (Fig. 4) allowed to chemically classify the waters in both seasons. In the dry period, the Laranjinha River waters were sodic, calcic (or magnesian) bicarbonated, while the Pedras stream waters were calcic (or magnesian) bicarbonated and sodic sulfated (or chlorinated). The groundwaters were mostly sodic sulfated (or chlorinated), followed by calcic (or magnesian) sulfated, chlorinated, or bicarbonated.

In the wet season, the Laranjinha River waters were calcic (or magnesian) bicarbonated while the Pedras stream waters were calcic (or magnesian) bicarbonated and sodic sulfated (or chlorinated). The groundwater samples were calcic, magnesian, or sodic sulfated (or chlorinated).

The Piper diagram indicates that CaMg becomes more common in groundwater in both periods, whereas the opposite for Na in the rainy period. This finding may reflect the increase of the dissolution rate due to chemical weathering in carbonate materials (rocks, soils, or even the carbonatic materials added in the reject dump). The Na concentration decrease would be caused by its higher dilution in waters during the

Table 3 Major anions in waters and effluents samples collected in August 2013

Sample	Chloride (mg L^{-1})	Bicarbonate (mg L^{-1})	Sulfate (mg L^{-1})	Nitrate (mg L^{-1})	Phosphate (mg L^{-1})
P1	1.30	50.0	4	1.5	4.00
P2	2.10	25.0	7875	5.0	1.20
P3	1.60	20.0	4521	64.0	5.20
P4	6.20	30.3	12,375	580.0	0.40
P5	0.90	15.0	1250	82.0	0.40
P6	1.40	70.0	3980	2.5	0.40
P7	2.10	15.0	200	1.5	0.80
P8	3.00	860.0	11,250	1.5	0.00
RP1	3.70	29.0	6	2.0	0.40
RP2	1.80	18.0	33	1.5	1.60
L1	1.50	42.0	14	2.5	0.20
L2	1.80	22.0	16	2.5	0.40
E1	0.20	4.0	4900	0.3	0.08
E2	2.25	1.0	9500	54.0	0.03

Table 4 Physico-chemical parameters for waters and effluents samples collected in February 2014

Sample	Temperature (°C)	pH	DO (mg L^{-1})	COD (mg L^{-1})	Conductivity (mS cm^{-1})	SS (mg L^{-1})	Eh (mV)
P1	25.2	5.45	5.85	42.24	0.03	786	268
P2	23.7	5.59	4.12	29.92	0.71	1519	441
P3	24.5	4.10	5.98	N.M.	1.53	1540	424
P4	24.3	3.25	2.49	181.28	4.47	1951	371
P5	24.2	4.46	1.12	1.76	1.20	7435	593
P6	26.4	4.50	5.82	N.M.	2.05	519	378
P7	23.3	3.90	5.41	N.M.	2.78	29	480
P8	25.0	6.63	3.37	26.4	5.50	280	−43
RP1	25.7	7.38	6.36	14.08	0.14	22	346
RP2	25.0	6.40	5.34	7.04	0.25	52	237
L1	26.7	7.59	6.59	5.28	0.06	5	387
L2	26.5	6.60	5.79	12.32	0.07	49	170
E1	26.4	4.30	2.58	190.08	4.54	175	341
E2	28.3	5.91	4.87	26.40	2.85	51	413

N.M. not measured

rainy period. In the dry period, higher Na concentration was also observed in waters from Pedras stream than in the wet period.

Equeenuddin et al. (2010) pointed out that natural waters chemically dominated by sulfate indicate a strong influence of AMD and this is the case for the groundwaters in this research. The bicarbonate predominance generally suggests that the waters are unaffected by AMD like observed for the Laranjinha River waters.

Chemical and spatial analysis of the AMD influences on the groundwater quality

The pH range of the groundwaters was 2.94 (P4)–6.04 (P8) and 3.25 (P4)–6.63 (P8) in the dry and wet periods, respectively. The more acid samples exhibited the highest concentrations of total iron (1010 and 1430 mg L^{-1}) and sulfate (12,375 and 14,400 mg L^{-1}).

Low pH and high SO_4^{2-} concentrations occur where the pyrite oxidation is pronounced that favors the calcite ($CaCO_3$) and dolomite ($CaMg(CO_3)_2$) dissolution from the rocks, increasing the concentrations of Ca and Mg in areas downstream the effluent discharge (Shim et al. 2015). On the other hand, limestone and dolomite have been used for neutralizing the AMD and precipitating metals (Genty et al. 2012).

The high SO_4^{2-}, Ca, and Mg levels in P4 and P5 in the rainy period possibly indicate a greater dissolution of minerals from Rio Bonito Formation during the wet season as a consequence of the water/soil-waste rock interactions.

Table 5 Major cations in waters and effluents samples collected in February 2014

Sample	Sodium (mg L^{-1})	Potassium (mg L^{-1})	Calcium (mg L^{-1})	Magnesium (mg L^{-1})	Ferrous iron (mg L^{-1})	Ferric iron (mg L^{-1})	Barium (mg L^{-1})	Aluminum (mg L^{-1})	Silica (mg L^{-1})
P1	2.21	0.92	2.80	1.00	0.02	0.27	4.5	0.10	19.0
P2	22.90	17.80	1.00	15.40	0.02	0.05	3.0	0.01	18.7
P3	15.00	3.60	16.00	12.00	0.20	1.00	3.0	0.20	15.0
P4	135.00	5.70	28.00	80.00	910.00	520.00	N.M.	4100.00	60.0
P5	24.30	25.20	240.00	100.00	72.00	116.00	120.0	80.00	21.1
P6	27.00	4.60	10.00	6.00	2.00	7.00	4.5	0.20	8.0
P7	89.00	3.20	6.00	6.00	3.00	4.00	3.0	0.10	6.0
P8	1009.00	36.40	0.40	0.20	28.00	57.00	1.5	N.M.	5.8
RP1	13.60	8.40	22.00	7.00	0.01	0.38	1.5	N.M.	17.3
RP2	14.20	6.92	0.60	1.20	0.01	0.16	3.0	0.04	14.8
L1	3.97	3.16	11.60	4.00	0.01	0.41	4.5	0.10	15.9
L2	4.19	3.44	12.00	2.02	0.01	0.40	1.5	0.14	16.2
E1	304.00	34.50	720.00	1240.00	1300.00	790.00	120.0	1132.00	3.1
E2	174.00	79.20	1.00	198.00	39.80	330.20	4.5	54.00	10.9

N.M. not measured

Table 6 Major anions in waters and effluents samples collected in February 2014

Sample	Chloride (mg L^{-1})	Bicarbonate (mg L^{-1})	Sulfate (mg L^{-1})	Nitrate (mg L^{-1})	Phosphate (mg L^{-1})
P1	10.8	20	1.5	1.8	0.20
P2	2.1	30	607.5	2.0	0.40
P3	7.8	15	175.0	1.0	2.00
P4	17.7	N.M.	14,400.0	N.M.	0.20
P5	14.1	N.M.	1550.0	28.5	0.40
P6	6.9	15	360.0	1.0	4.00
P7	4.5	10	320.0	0.5	3.00
P8	3.6	420	8300.0	N.M.	0.40
RP1	4.8	60	30.0	2.5	0.40
RP2	N.M.	30	46.0	2.5	0.20
L1	3.9	75	3.0	2.5	0.20
L2	4.8	70	12.0	3.5	0.80
E1	7.2	5	14,700.0	160.0	0.20
E2	1.8	3	3400.0	5.0	0.20

N.M. not measured

In the rainy period, the groundwater samples exhibited higher mean values for temperature (14 %), EC (21 %), pH (15 %), COD (68 %), SS (2 times), chloride (4 times), and Fe^{2+} (20 times) compared to those of the dry season. The highest Fe^{2+} concentration in groundwaters in the rainy month indicates a higher AMD generation from the sulfide minerals' oxidation. The higher COD concentration and SS can be due to the higher amount of organic matter and other compounds leached and transported by rainwater.

However, some parameters exhibited lower mean values in the rainy month: DO (28 %), magnesium (6 times), bicarbonate (2 times), sulfate (2 times), nitrate (21 times), Fe^{3+} (2.5 times), barium (4 times), and aluminum (2 times). Dilution processes in the period of the highest aquifer recharge could justify these lower concentrations. Sodium, potassium, calcium, phosphate, and silica did not exhibit a pronounced variation in the monitored periods. The results found for Fe^{2+} and SO_4^{2-} (lower and higher in the dry season, respectively) were opposite of those reported by Sun et al. (2013) in AMD-impacted water.

Shim et al. (2015) suggested that it is unlikely that the long-term decreases in major ions were only because their samples were taken during the rainy season. Processes like dilution by mixing, co-precipitation/adsorption and changes in the Eh and pH could also control the spatial distribution of cations and anions in AMD-affected waters. Perhaps, they could justify the lower average concentration levels of sulfate and some metals in groundwater in the wet period.

Results found by Cravotta (2008) show that the water chemistry could be explained by dilution and neutralization

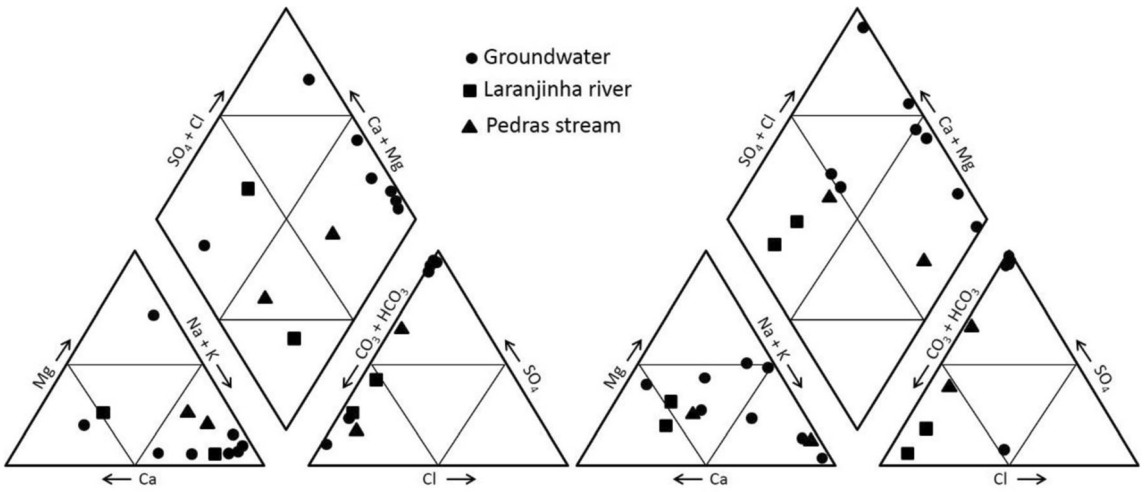

Fig. 4 Piper (1944) diagram for river and groundwater samples collected in August 2013 and February 2014

of acid waters, solubility limits of Al, Fe, and other metal precipitates, sulfate complexation, sorption reactions, and carbonate-buffered groundwaters. In the study area, the pH correlated with bicarbonate, accompanying the chemical balance of bicarbonate in acid solution (Eq. 5). For both periods, pH and Log [HCO_3^{-1}] exhibited a significant correlation (Fig. 5).

$$HCO_{3^-(aq)} + H^+_{(aq)} \rightarrow H_2O_{(l)} + CO_{2(aq)} \quad (5)$$

Dissolution of mineral phases along the water flow in the aquifer can buffer the pH of the acidic effluent up to neutral conditions (Benner et al. 2000). In the dry period, bicarbonate concentrations ranged from 15 to 860 mg L^{-1} (mean = 135.7 mg L^{-1}). The highest bicarbonate concentration was in sampling point P8 (both seasons). Candeias et al. (2014) pointed out that the increasing metal content with decreasing pH reflects the greater sulfide minerals' oxidation and a smaller content of carbonates/aluminosilicates consuming the acidity (Arnold et al. 1988). Such finding can explain the lower bicarbonate content in the groundwaters in the wet period when the AMD production was greater and accompanied by higher Ca and Mg concentrations in some samples.

No significant variation was found in Log [HCO_3^{-1}] and pH of the groundwaters in both seasons (Fig. 5). The higher AMD production due to a more accentuated oxidation of sulfide minerals and dissolution of some constituents could justify the increase of the buffering capacity during the wet period. However, the low pH (<4 in most of the samples) and the presence of high levels of metals in solution suggests the occurrence of sulfide minerals oxidation, indicating inefficient neutralization by the carbonate materials from Rio Bonito Formation and/or from the materials (CaO) added in the tailings pile in order to control the acidity (Campaner and Luiz-Silva 2009). Despite the dissolution of calcite and other carbonates could buffer the pH of the groundwater surrounding the tailings pile and neutralize the AMD (Malmstro et al. 2008), such process is not successful there.

In the dry period, temperature correlated inversely with DO (Pearson correlation coefficient $r = -0.96$) in groundwaters, indicating less oxygen in the waters at more elevated temperatures. Temperature in the dry period correlated directly with EC ($r = 0.82$), Na ($r = 0.97$), Ca ($r = 0.95$), Mg ($r = 0.97$), and HCO_3^- ($r = 0.97$), suggesting that they are more solubilized when the water temperature increases. The inverse relationship between temperature and DO implied inverse significant correlations of DO with Na ($r = -0.98$), K ($r = -0.76$), Ca ($r = -0.96$), Mg ($r = -0.98$), and HCO_3^- ($r = -0.98$). The following direct correlations were also found in the dry season: Na with Ca ($r = 0.98$), Mg ($r = 0.99$), and HCO_3^- ($r = 0.99$); Ca with HCO_3^- ($r = 0.98$); Mg with HCO_3^- ($r = 1.0$); and K with Ca ($r = 0.78$). They indicate that their leaching from rocks and soils is catalyzed with the increase in the temperature.

During the rainy season, the groundwater pH correlated inversely with silica ($r = -0.92$) and chloride ($r = -0.88$), indicating that the more acid conditions favor the leaching of the aquifer rocks. Eh correlated inversely with bicarbonate ($r = -0.88$), suggesting a lowering of the redox conditions with increasing the alkalinity. The suspended solids correlated directly with Ca ($r = 0.99$), Ba ($r = 0.97$), and NO_3^- ($r = 0.97$), indicating congruent dissolution processes affecting the particulate matter and dissolved constituents. The following direct correlations were also found in the wet season: Na with HCO_3^- ($r = 0.99$); Ba with NO_3^- ($r = 1.00$) and Ca ($r = 0.99$); Fe^{2+} with Fe^{3+} ($r = 0.99$), Al ($r = 1.0$), and SiO_2 ($r = 0.96$); Fe^{3+} with Al ($r = 0.98$) and Ba ($r = 0.93$); COD with Fe^{2+} ($r = 0.96$), Fe^{3+} ($r = 0.91$), and Al ($r = 0.97$). These relationships suggest that the dissolved organic matter concentration affects the water pH due to the organic acid formation and, as a consequence, the acidity increase enhances the dissolved iron concentration.

The spatial data representation in Figs. 6 and 7 shows that DO in the dry season increased at the sampling point P1 and that pH became more acidic downstream the mine, according to the groundwater flow direction. The concentrations of sulfate and dissolved iron at the sampling points P3, P4, P5, and E2 were high

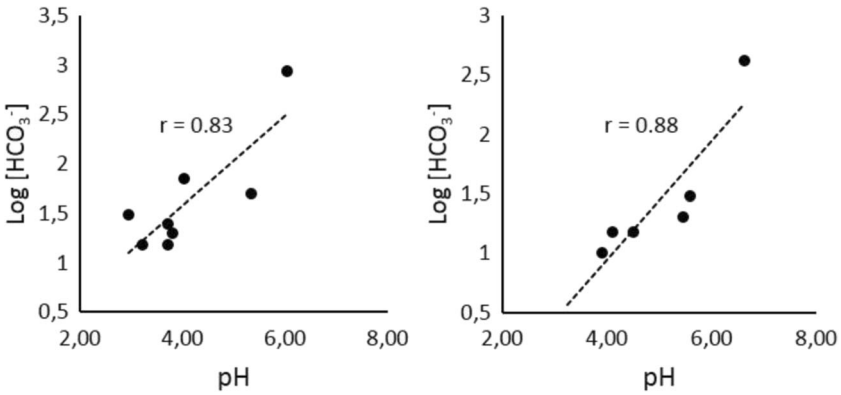

Fig. 5 Relations between pH and bicarbonate for groundwaters collected in August 2013 (*left*) and February 2014 (*right*)

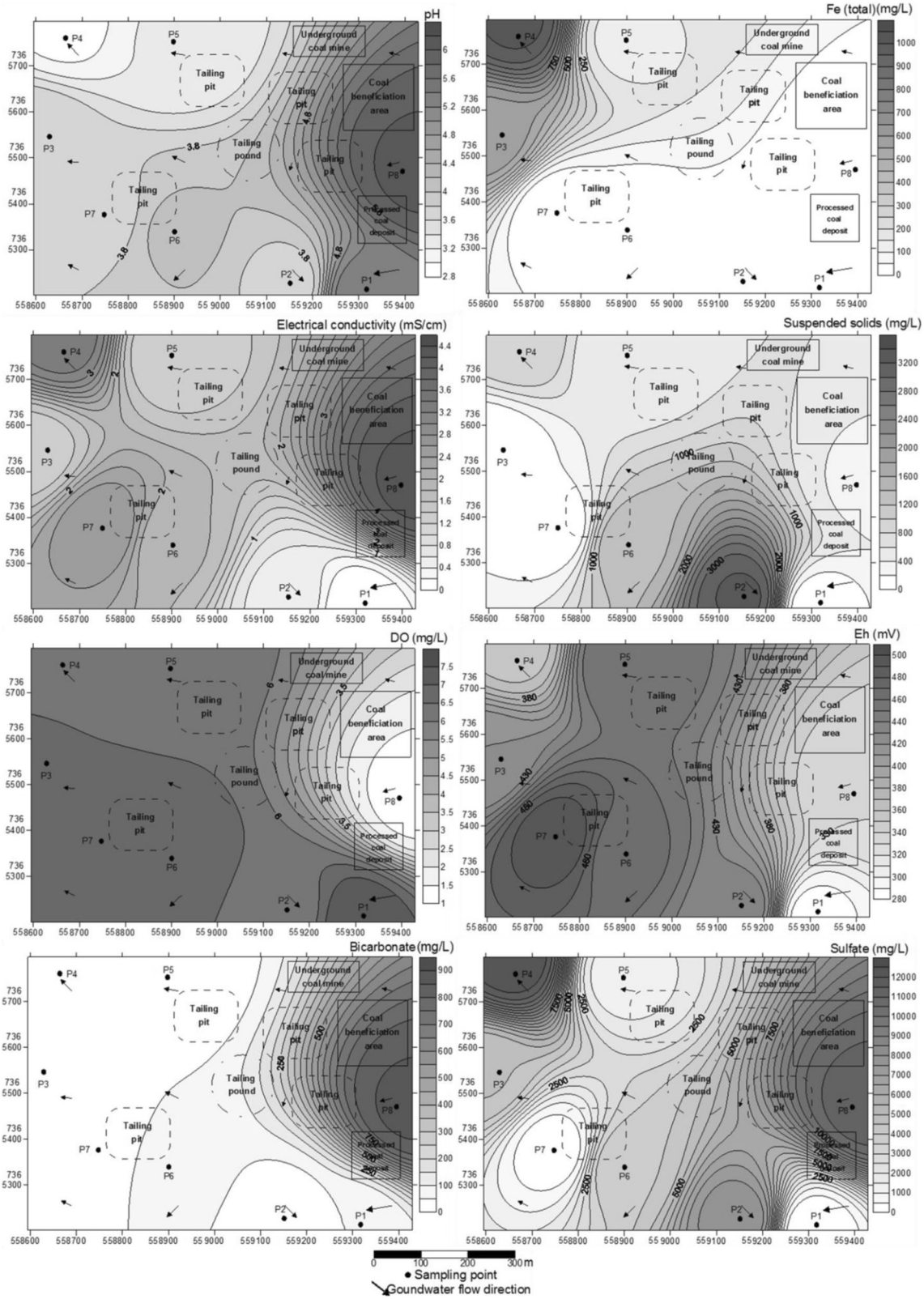

Fig. 6 Spatial distribution of EC, SS, DO, Eh, pH, iron (total), sulfate, and bicarbonate in groundwaters collected in August 2013

due to the low pH values, indicating the AMD influence there. The sulfate spatial distribution shows a pattern similar to EC (Figs. 6 and 7). The bicarbonate concentrations were high in the coal processing area and

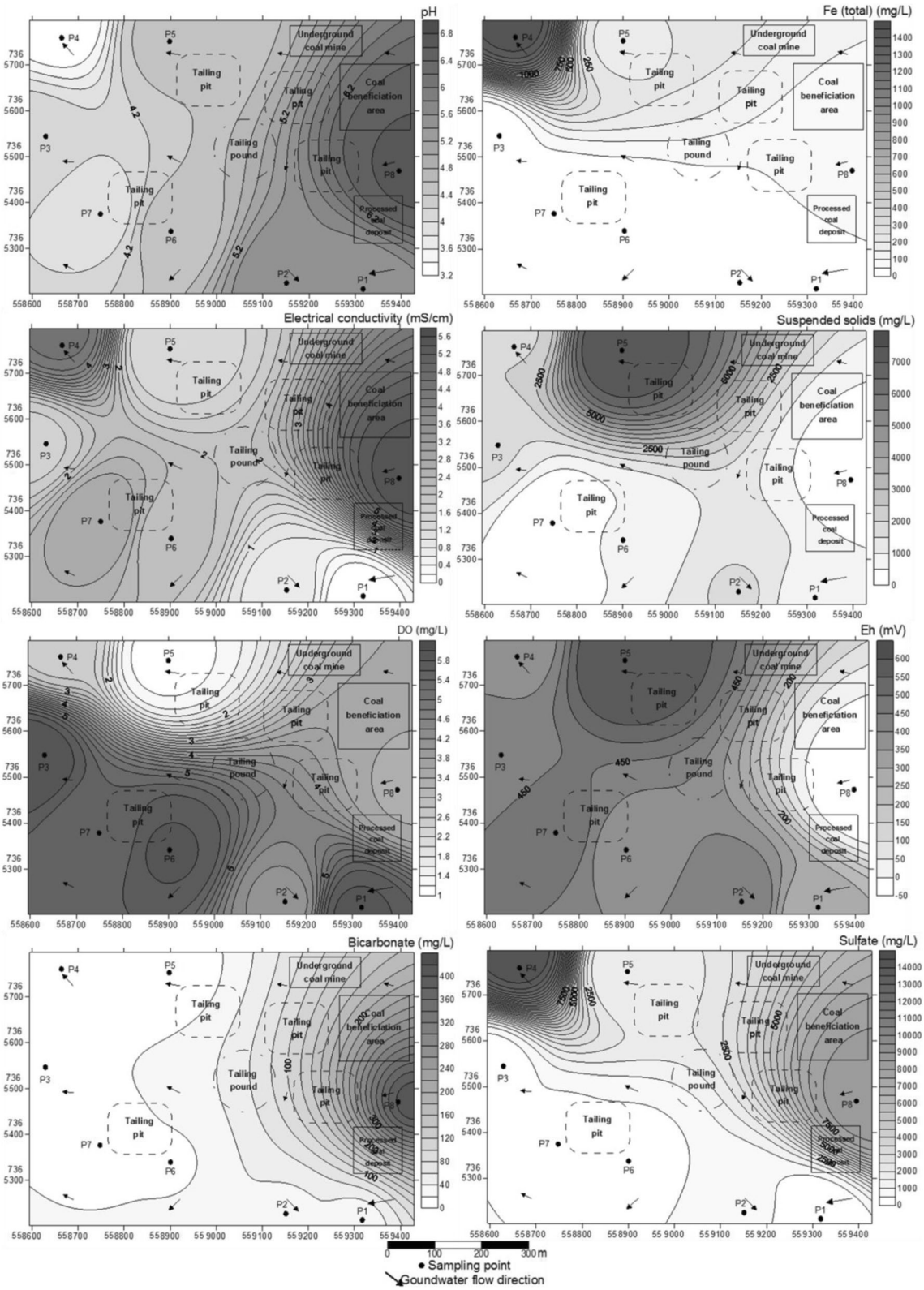

Fig. 7 Spatial distribution of EC, SS, DO, Eh, pH, iron (total), sulfate, and bicarbonate in groundwaters collected in February 2014

tailings in both monitoring periods, agreeing with the pH distribution in the area that was less acidic where HCO_3^- was higher.

In the dry period, the SS exhibited high values in P2 (3239 mg L^{-1}), P4 (993 mg L^{-1}), and P6 (1364 mg L^{-1}) that are located downstream the mining area. The sampling point

P8 is between the reject dumps and the coal processing area, exhibiting high levels for Na (859 mg L^{-1}), Mg (1400 mg L^{-1}), Ca (196 mg L^{-1}), HCO_3^- (860 mg L^{-1}), and SO_4^{2-} (11,250 mg L^{-1}). The sulfate concentration was also high at P2 (7875 mg L^{-1}), P3 (4521 mg L^{-1}), P4 (12,375 mg L^{-1}), P5 (1250 mg L^{-1}), P6 (3980 mg L^{-1}), and for both effluent samples. They confirm the occurrence of AMD and acid effluent transport to groundwater as corroborated by the high Fe^{3+} concentration in P3 (566 mg L^{-1}), P4 (988 mg L^{-1}), P5 (131 mg L^{-1}), and E2 (2824 mg L^{-1}), as well as the high Al concentration in P2 (2080 mg L^{-1}), P3 (1067 mg L^{-1}), P4 (2542 mg L^{-1}), P6 (1090 mg L^{-1}), and E2 (1318 mg L^{-1}).

The acid waters can be displaced/discharged into adjacent geological materials/surface water flow systems (Candeias et al. 2014), but their main route in the study area is the local aquifer due to the effluent percolations associated to the tailings disposal in its recharge zone. Iron, aluminum, and other elements can migrate downward through the vadose zone towards the water table (Gunsinger et al. 2006) and the low pH conditions can also promote the dissolution of many metal-bearing solids and the metal desorption from solid surfaces in the aquifer matrix (Candeias et al. 2014). Gunsinger et al. (2006) suggest that strategies for AMD remediation should focus on the mitigation of dissolved constituents rather than on preventing further sulfide oxidation in mining areas. This is because high H^+ levels will migrate downward from surface, decreasing the pore waters' pH and favoring the metals' solubilization due to depletion of carbonate and other neutralizing minerals.

In the rainy period, EC and SS were lower mainly next to the sampling points P2, P6, and P7. The highest pH values were downstream and next to the mine plant. High total iron concentration was found where the groundwater exhibited the lowest pH value. High SS concentrations were measured in the sampling points P2 to P5, downstream the mine. The following high concentrations were also found: Na (1009 mg L^{-1}), HCO_3^- (420 mg L^{-1}), and SO_4^{2-} (8300 mg L^{-1}) in P8; Ca (240 mg L^{-1}) and SO_4^{2-} (1550 mg L^{-1}) in P5; Al (4100 mg L^{-1}), SO_4^{2-} (14,400 mg L^{-1}), Fe^{2+} (910 mg L^{-1}), and Fe^{3+} (520 mg L^{-1}) in P4; SO_4^{2-} (14,700 mg L^{-1}), Fe^{3+} (790 mg L^{-1}), Fe^{2+} (1300 mg L^{-1}), and Al (1132 mg L^{-1}) in E1 and SO_4^{2-} (3400 mg L^{-1}) in E2.

Another relevant aspect is that, in addition to pyrite oxidation, the low pH values allow the dissolution of aluminosilicate minerals as observed by the high concentration of SiO_2 in some groundwater samples, for instance, P3 in August 2013 (105.60 mg L^{-1}) and P4 in February 2014 (60.00 mg L^{-1}). Likewise, the high Na concentration in P8 (August 2013 = 859.00 mg L^{-1}; February 2014 = 1009.00 mg L^{-1}) suggests that the dissolution of clay minerals/aluminosilicates is taking place there.

AMD effects on surface waters and effluents

The pH values decreased and the SO_4^{2-} concentration increased downstream the mine for both Laranjinha River and Pedras stream in the dry and wet seasons. Candeias et al. (2014) reported a near neutral pH and low metal concentrations in upstream water samples collected at Zêzere River, Portugal. The pH downstream Laranjinha River (L2) was more acidic than upstream (L1) for both seasons possibly due to mixing of waters from Pedras stream that is located closer to the mine; thus, more favorable to receive the acid effluents from the mining activities.

The EC and SS values were higher downstream Laranjinha River and Pedras stream (L2 and RP2, respectively) in the dry season. They reflect the interaction of the surface waters with the acid effluents generated during the mining activities as a consequence of the runoff and effluents transport. In Pedras stream, Na, K, Mg, Al, SiO_2, SO_4^{2-}, and PO_4^{3-} and in Laranjinha River, COD, Na, K, Ca, Mg, Fe^{3+}, Cl^-, SO_4^{2-}, and PO_4^{3-} were higher downstream the mine. In the rainy season, both waters exhibited more acidity, lower EC and DO and higher SS, Na, and SO_4^{2-} concentrations downstream the mine, whereas, in Laranjinha River, K, Ca, SiO_2, Cl, NO_3^-, and PO_4^{3-} were higher downstream the mining area.

The effluent samples exhibited higher temperatures compared to river and groundwater samples. In the dry season, the acidity, EC, DO, COD, Fe^{2+}, Fe^{3+}, Al, Ba, Ca, Cl, and SO_4^{2-} were lower in E1 than in E2, although no CaO was added to the pH control in E1. This database may indicate a lower AMD generation and metals leaching in the oldest reject dump, followed by a higher metals immobilization in solution due to a chemical stabilization over the time. In the rainy season, in a different way, the acidity, Fe^{2+}, Fe^{3+}, SO_4^{2-}, Cl, HCO_3^-, NO_3^-, Na, Ca, Mg, Ba, and Al were higher in E1 than in E2, possibly due to a higher AMD production in the wettest period. This would favor the dissolution processes affecting, for instance, clay minerals and phyllosilicates, promoting the release of Na, Cl, and other constituents.

AMD indicators

Several environmental problems occur when AMD flows into groundwater, streams, or rivers. The toxic mixtures bring effects to natural waters that are related to the property of heavy metals to persist in the ecosystems for an extended period, accumulating in successive levels of the biological chain (Simate and Ndlovu 2014). Although this process occurs naturally, mining activities accelerate the AMD generation and, consequently, the water contamination as occurring in the study area. Some indicators based on chemical relations can help on the monitoring of the water pollution caused by the AMD generation. In the driest month, low pH and high iron and sulfate concentrations point out that pyrite oxidation

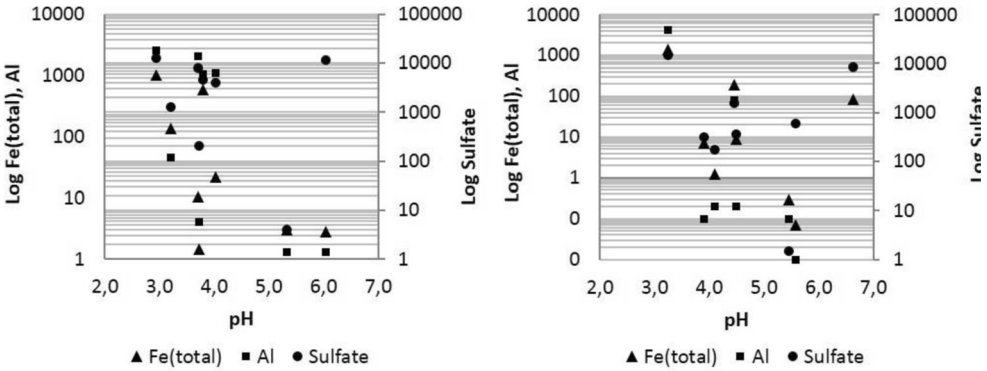

Fig. 8 Relations between pH, total iron, aluminum, and sulfate content for groundwaters collected in August 2013 (*left*) and February 2014 (*right*)

occurs (Candeias et al. 2014). This situation was found in the sampling points P2 to P8 and E1 and E2.

However, neutralization also occurs besides the groundwater acidification. Dilution processes and/or background values of groundwaters would justify the low metal concentration and neutral pH of the waters investigated by Candeias et al. (2014), but this was not the case of the waters in this research. Once formed, the AMD interaction with alkaline materials may provide the metal removal by their precipitation in solution. Waters with high sulfate concentration and lower iron levels can be indicative of AMD previously generated but controlled over the time. This neutral mine drainage refers to drainage waters mainly exhibiting pH 6–9 and high levels of dissolved sulfate and trace metals derived from sulfide oxidation (Nordstrom et al. 2015). Such condition was observed in some sites of the study area as the acid neutralization capacity related to the carbonate minerals was greater than the acid generated due to the AMD. For instance, in the dry month, P1 and P8 relatively to other groundwater monitoring points were less acidic (pH = 5.34 and 6.04), exhibited lower total Fe (3.01 and 2.80 mg L^{-1}) and Al (1.3 mg L^{-1}), and higher HCO_3^- (50 and 860 mg L^{-1}). The AMD neutralization can be verified in the sampling points P2, P3, P6, and P7 that exhibited high sulfate and low iron concentrations.

Iron will precipitate if pH is above or close to 3.5 (Al-Hashimi et al. 1996; Chen et al. 2014), whereas at pH below 3.5, a few or no iron precipitation occurs (Al-Hashimi et al. 1996). However, at pH values near or below 3.5, Fe(III) concentration increases in solution, acting as an oxidizing agent for pyrite in AMD (Lottermoser 2010). In both periods, the lower iron concentration in some sampling points (such as P1, P2, P3, P6, and P7 in the wet period) may be due its precipitation in the (hydr)oxide forms as Fe^{3+} showed a slight upward trend with the pH decreasing in the groundwaters (the Pearson correlation coefficient was −0.51 and −0.52). This is comparable to the results described by Liao et al. (2016) who found in waters contaminated by acid effluents a decrease in the Fe(III) concentration with the pH rising.

In the study area, lower iron concentrations in groundwater were found at pH >3 and, in the dry period, there is a slight upward trend in iron and aluminum concentrations with the water acidification (Fig. 8). In the rainy period, the lower iron concentrations were found at pH >4, a slight upward trend in the sulfate, aluminum, and iron concentrations with the increased acidification was also observed. The Al concentrations decreased at P1 and P8 (dry month) and P1 and P2 (wet month), probably due to the pH increase, resulting in significant Al precipitation. Other metals and elements can be removed by adsorption/co-precipitation with Fe and Al precipitates (Shim et al. 2015). In addition to the increase in total iron and sulfate with the sample's acidification, in the dry period, the pH rises with the bicarbonate concentration in the groundwater samples (Fig. 9). Such trend was less pronounced in the rainy period.

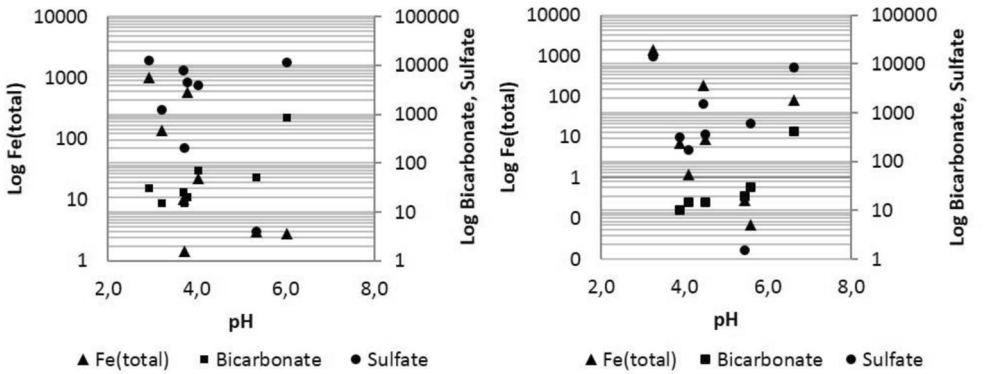

Fig. 9 Relations between pH, total iron, bicarbonate, and sulfate content for groundwaters collected in August 2013 (*left*) and February 2014 (*right*)

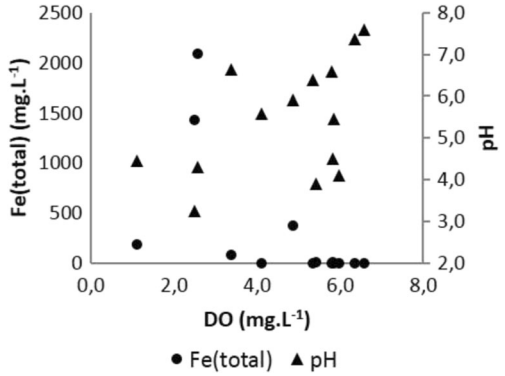

Fig. 10 Relations between pH, total iron, and DO for samples collected in February 2014

Oxygen is the ultimate oxidant of sulfide minerals in natural surface systems but, at pH <4, sulfides can be oxidized by Fe^{3+}. Sulfide oxidation generally occurs in areas where the DO is present, as oxygen is the primary oxidizing agent for Fe^{2+} to Fe^{3+} (Benner et al. 2000). In poorly oxygenated waters, pyrite oxidation can occur slowly, reflecting on the pH solutions. Waters with reduced DO and Fe(III) do not favor pyrite oxidation, implying on the pH data, which turns less acidic. A slight upward trend for both pH and total iron with DO was found in the rainy period (Fig. 10).

Gray (1996) proposed that conductivity and sulfate levels could act as AMD indicators from data obtained in a copper mine area in Ireland that consisted of contaminated surface waters with AMD influence, surface runoff, and leachate stream. This is based on the fact that the sulfate minerals provide a source of acidity and dissolved metals to the mine drainage and may be associated with mine wastes and processes, providing pollutants to the mine waters (Nordstrom et al. 2015). In this research, SO_4^{2-} and EC were correlated, like Na and EC. Using regression analysis, relationships between SO_4^{2-} and EC are given in Table 7 for both sampling periods. Diverse climatic conditions, lithologies and minerals assemblage could explain the different equation reported by Gray (1996): Log $[SO_4^{2-}] = 1.51 \times$ Log (EC) − 1.85 ($r^2 = 0.98$). In tropical areas, chemical weathering is sometimes favored in relation to processes occurring in temperate ones, implying increase in the EC. Chalcopyrite ($CuFeS_2$) and other sulfide minerals containing Fe, Cu, As, Sb, Bi, Se, and Mo can originate acid solutions; however, they are not commonly associated with coal horizons (Berghorn and Hunzeker 2001), principally at the Figueira coal deposit where main mineral phase is pyrite (FeS_2).

Significant correlation was found among EC, SO_4^{2-}, and Na in most cases for both seasons. Pure water has low EC values that increase significantly with the electrolytes addition. Sodium is an important hydrochemical analyte in Figueira city, whose concentration in groundwater ranged in different orders of magnitude in both seasons as a

Table 7 Regression equations with sulfate, conductivity, sodium, and iron concentrations

August 2014		February 2014	
Total samples (surface and groundwater + AMD)			
Linear regression	r^2	Linear regression	r^2
$Log[SO_4^{2-}] = 1.56 \times LogConductivity + 3.06$	0.81	$Log[SO_4^{2-}] = 1.59 \times LogConductivity + 0.65$	0.89
$Log[Fe_{(total)}] = 1.26 \times LogConductivity + 1.21$	0.42	$Log[Fe_{(total)}] = 1.52 \times LogConductivity + 1.04$	0.58
$Log[Na] = 0.80 \times LogConductivity + 1.65$	0.73	$Log[Na] = 0.89 \times LogConductivity + 1.63$	0.81
$Log[SO_4^{2-}] = 0.67 \times Log[Fe_{(total)}] + 2.08$	0.57	$Log[SO_4^{2-}] = 0.70 \times Log[Fe_{(total)}] + 1.85$	0.69
$Log[SO_4^{2-}] = 1.52 \times Log[Na] + 0.48$	0.68	$Log[SO_4^{2-}] = 1.56 \times Log[Na] + 0.09$	0.83
Groundwater + AMD			
Linear regression	r^2	Linear regression	r^2
$Log[SO_4^{2-}] = 1.31 \times LogConductivity + 3.18$	0.67	$Log[SO_4^{2-}] = 1.63 \times LogConductivity + 2.62$	0.82
$Log[Fe_{(total)}] = 0.58 \times LogConductivity + 1.56$	0.12	$Log[Fe_{(total)}] = 1.57 \times LogConductivity + 1.05$	0.45
$Log[Na] = 0.65 \times LogConductivity + 1.72$	0.51	$Log[Na] = 0.10 \times LogConductivity + 1.57$	0.75
$Log[SO_4^{2-}] = 0.47 \times Log[Fe_{(total)}] + 2.53$	0.25	$Log[SO_4^{2-}] = 0.60 \times Log[Fe_{(total)}] + 2.12$	0.61
$Log[SO_4^{2-}] = 1.14 \times Log[Na] + 1.28$	0.42	$Log[SO_4^{2-}] = 1.37 \times Log[Na] + 0.52$	0.77
Surface water + AMD			
Linear regression	r^2	Linear regression	r^2
$Log[SO_4^{2-}] = 1.76 \times LogConductivity + 3.05$	0.95	$Log[SO_4^{2-}] = 1.77 \times LogConductivity + 2.87$	0.98
$Log[Fe_{(total)}] = 2.05 \times LogConductivity + 1.39$	0.73	$Log[Fe_{(total)}] = 2.06 \times LogConductivity + 1.59$	0.88
$Log[Na] = 0.95 \times LogConductivity + 1.68$	0.98	$Log[Na] = 0.98$ x $LogConductivity + 1.82$	0.99
$Log[SO_4^{2-}] = 0.67 \times Log[Fe_{(total)}] + 1.91$	0.79	$Log[SO_4^{2-}] = 0.76 \times Log[Fe_{(total)}] + 1.56$	0.89
$Log[SO_4^{2-}] = 1.81 \times Log[Na] - 0.01$	0.93	$Log[SO_4^{2-}] = 1.78 \times Log[Na] - 0.38$	0.98

Level of significance alpha = 0.050; $[SO_4^{2-}]$, [Fe(total)], [Na] = mg L^{-1}; Conductivity = mS cm^{-1}

consequence of water/soil-waste rock interactions, water flow rate, recharge rate, and acid solutions infiltration. The applicability of sodium as an indicator of water pollution must take into account the background values of this element in rivers and groundwater. In some cases, the correlation between Na and SO_4^{2-} in groundwaters and surface waters (Table 7) suggests their use as potential AMD indicators at Figueira city.

Despite total Fe exhibiting significant correlation with EC and SO_4^{2-} in surface waters, its use as an AMD indicator shall be better investigated, mainly because of the lack of a significant correlation among them in groundwater. Depending on pH, some iron may be in the precipitated form, not remaining in solution. For instance, in surface waters, the pH >6 allows the iron precipitation in both sampling periods. Furthermore, an increase in total iron content was not observed downstream in relation to the monitoring point located upstream the mining area.

Final considerations

The results of this research indicate that acid effluents are originated by the coal mining activities held at Figueira city, Paraná State, Brazil, enhancing the iron and aluminum leaching and transport from the reject dumps into the aquifer and superficial water bodies. The effluents' acidification affected by pyrite oxidation may result in an increase of the metals' solubilization, favoring the soil and groundwater contamination up to levels of difficult treatment and recovery, where the iron concentration was very high (e.g., sampling points P3 and P4 in the dry and wet seasons). The chemistry of groundwaters and surface waters in the vicinity of the coal mining is controlled and influenced by seasonal variations, which allows processes of dissolution and concentration of some constituents. The seasonal climate variations also increase or decrease the metal leaching from rocks, soils, or tailing piles, affecting the sulfide minerals oxidation, dissolved oxygen, iron concentrations, water's pH, and microbial activity, i.e., the acid mine drainage (AMD) generation and extension through the waters. Different chemical stages of the AMD influences on the groundwater composition have been identified. Firstly, highly acidic effluents are generated in some monitoring points, causing a pH decrease in the solution and an increase in the concentrations of sulfate and some dissolved cations. In the next step, the pH is modified due to interactions with alkaline materials, thus, less acidic solution gives rise to lower levels of dissolved metals. Sulfate remains in high levels as it is more stable to the pH changes and together with sodium and electrical conductivity (EC) they could be used for evaluating the water quality. Among them, EC is a low-cost parameter and easy to determine in the field, giving a first overview of the water quality in a river or stream. For reliable results, it is recommended to monitor the parameters in more than one hydrological cycle, what enables greater control over the involved variables. Similarly, heavy and toxic metal attenuation comprises complex processes involving AMD and adsorption, co-precipitation, and transformation reactions. Therefore, further studies are required in the study area, considering the seasonal climate variations. They would enable a greater control over the environmental damage, helping to understand the AMD effects on waters used for human consumption, thus, contributing to the environmental preservation.

Acknowledgments CNPq (National Council for Scientific and Technologic Development) in Brazil is thanked for financial support of this investigation. Three anonymous reviewers are greatly thanked for helpful comments that improved the readability of the manuscript.

References

Akcil A, Koldas S (2006) Acid mine drainage (AMD): causes, treatment and case studies. J Clean Prod 14:1139–1145. doi:10.1016/j.jclepro.2004.09.006

Al-Hashimi A, Evans GJ, Cox B (1996) Aspects of the permanent storage of uranium tailings. Water Air Soil Pollut 88:83–92. doi:10.1007/BF00157414

ANEEL (Agência Nacional de Energia Elétrica) (2011) A Situação da Produção de Carvão Mineral no Estado do Paraná em Relação a Nota Técnica 034/2011. Tech. Rep, ANEEL, Brasília

Arnold T, Zorn T, Zänker H, Bernhard G, Nitsche H (1988) Sorption of U(VI) onto phyllite: experiments and modeling. Chem Geol 151:129–141. doi:10.1016/S0169-7722(00)00151-0

Baik MH, Hyun SP, Hahn PS (2003) Surface and bulk sorption of uranium (VI) onto granite rock. J Radioanal Nucl Chem 256:11–18. doi:10.1023/A:1023331521718

Benner SG, Gould WD, Blowes DW (2000) Microbial populations associated with the generation and treatment of acid mine drainage. Chem Geol 169:435–448

Berghorn GH, Hunzeker GR (2001) Passive treatment alternatives for remediating abandoned mine drainage. Remediat J 11:111–127. doi:10.1002/rem.1007

Bizzi LA, Schobbenhaus C, Vidotti RM, Gonçalves JH (2003) Geologia, Tectônica e recursos Minerais do Brasil: texto, mapas e SIG. CPRM, Brasília

Blowes DW, Ptacek CJ, Jambor JL, Weisener CG, Paktunc D, Gould WD, Johnson DB (2014) The geochemistry of acid mine drainage. Reference module in earth systems and environmental sciences. Treatise Geochem 11:131–190. doi:10.1016/B978-0-08-095975-7.00905-0

Bonotto DM (1996) Comportamento hidrogeoquímico do 222Rn e isótopos de urânio 238 U e 234 U sob condições controladas de laboratório e em sistemas naturais. Post PhD Thesis, UNESP, Rio Claro

Campaner VP, Luiz-Silva W (2009) Processos físico-químicos em drenagem ácida de mina em mineração de carvão no sul do Brasil. Quim Nov. 32:146–152. doi:10.1590/S0100-40422009000100028

Campaner VP, Luiz-Silva W, Machado W (2014) Geochemistry of acid mine drainage from a coal mining area and processes controlling metal attenuation in stream waters, southern Brazil. An Acad Bras Ciênc 86:539–554. doi:10.1590/0001-37652014113712

Candeias C, Ávila PF, Silva EF, Ferreira A, Salgueiro AR, Teixeira JP (2014) Acid mine drainage from the Panasqueira mine and its influence on Zêzere river (Central Portugal). J Afr Earth Sci 99:705–712. doi:10.1016/j.jafrearsci.2013.10.006

Caraballo MA, Macías F, Nieto JM, Ayora C (2016) Long term fluctuations of groundwater mine pollution in a sulfide mining district with dry Mediterranean climate: implications for water resources management and remediation. Sci Total Environ 539:427–435. doi:10.1016/j.scitotenv.2015.08.156

Carrero S, Pérez-López R, Fernandez-Martinez A, Cruz-Hernández P, Agnieszka CA, Ayora C, Poulain A (2015) The potential role of aluminium hydroxysulphates in the removal of contaminants in acid mine drainage. Chem Geol 417:414–423. doi:10.1016/j.chemgeo.2015.10.020

Chen T, Bo Y, Lei C, Xiao X (2014) Pollution control and metal resource recovery for acid mine drainage. Hydrometallurgy 147–148:112–119. doi:10.1016/j.hydromet.2014.04.024

CONAMA (Conselho Nacional do Meio Ambiente) (2005) Rule 357 published in 17th Mar 2005. http://www.mma.gov.br/port/conama/res/res05/res35705.pdf

CONAMA (Conselho Nacional do Meio Ambiente) (2011) Rule 430 published in 13th May 2011. http://www.mma.gov.br/port/conama/res/res11/propresol_lanceflue_30e31mar11.pdf

Cravotta CA (2008) Dissolved metals and associated constituents in abandoned coal-mine discharges, Pennsylvania, USA. Part 2: geochemical controls on constituent concentrations. Appl Geochem 23:203–226

Equeenuddin SM, Tripathy S, Sahoo PK, Panigrahi MK (2010) Hydrogeochemical characteristics of acid mine drainage and water pollution at Makum coalfield, India. J Geochem Explor 105:75–82. doi:10.1016/j.gexplo.2010.04.006

Francis AJ (1990) Microbial dissolution and stabilization of toxic metals and radionuclides in mixed wastes. Experientia 46:840–851. doi:10.1007/BF01935535

Fungaro DA, Izidoro JC (2006) Remediação da drenagem ácida de mina usando zeólitas sintetizadas a partir de cinzas leves de carvão. Quim Nov. 29:735–740. doi:10.1590/S0100-40422006000400019

Geldenhuis S, Bell FG (1998) Acid mine drainage at a coal mine in the eastern Transvaal, South Africa. Environ Geol 34:234–242. doi:10.1007/s002540050275

Genty T, Bussiere B, Potvin R, Benzaazoua M, Zagury GJ (2012) Dissolution of calcitic marble and dolomitic rock in high iron concentrated acid mine drainage: application to anoxic limestone drains. Environ Earth Sci 66:2387–2401. doi:10.1007/s12665-011-1464-3

Gray NF (1996) Field assessment of acid mine drainage contamination in surface and ground water. Environ Geol 27:358–361. doi:10.1007/BF00766705

Gunsinger MR, Ptacek CJ, Blowes DW, Jambor JL (2006) Evaluation of long-term sulfide oxidation processes within pyrrhotite-rich tailings, Lynn Lake, Manitoba. J Contam Hydrol 83:149–170. doi:10.1016/j.jconhyd.2005.10.013

Krebs ASJ, Alexandre NZ (1998) Situação atual dos recursos hídricos da bacia carbonífera, face às atividades de lavra, beneficiamento e uso do carvão mineral e de outras atividades antrópicas. Proceedings of IX Congresso Brasileiro de Águas Subterrâneas, Bahia, pp 60–65

Küsel K (2003) Microbial cycling of iron and sulfur in acid coal mining lake sediments. Water Air Soil Pollut 3:67–90. doi:10.1023/A:1022103419928

Liao J, Wen Z, Ru X, Chen J, Wu H, Wei C (2016) Distribution and migration of heavy metals in soil and crops affected by acid mine drainage: public health implications in Guangdong Province, China. Ecotoxicol Environ Saf 124:460–469. doi:10.1016/j.ecoenv.2015.11.023

Licht OAB (2001) Atlas geoquímico do Paraná. Mineropar, Curitiba

Lee MH, Choi CS, Cho YH, Lee CW, Shin HS (2001) Concentrations and activity ratios of uranium isotopes en the groundwater os the Okchum Belt in Korea. J Environ Radioact 55:105–116. doi:10.1016/S0265-931X(01)00014-5

Lottermoser B (2010) Mine wastes: characterization, treatment and environmental impacts, 3rd edn. Springer, Berlin. doi:10.1007/978-3-642-12419-8

Malmstro ME, Berglund S, Jarsjo J (2008) Combined effects of spatially variable flow and mineralogy on the attenuation of acid mine drainage in groundwater. Appl Geochem 23:1419–1436. doi:10.1016/j.apgeochem.2007.12.029

MINEROPAR (Minerais do Paraná) (2001) Diagnóstico preliminar dos impactos ambientais da mineração no Paraná. Mineropar, Curitiba

Molson J, Aubertin M, Bussière B (2012) Reactive transport modelling of acid mine drainage within discretely fractured porous media: plume evolution from a surface source zone. Environ Model Softw 38:259–270. doi:10.1016/j.envsoft.2012.06.010

Nordstrom DK, Alpers CN (1999) Geochemistry of acid mine waters. In: Plumlee GS, Logsdon M (eds) Society & Economic Geologists 6 A 133–160

Nordstrom DK (2009) Acid rock drainage and climate change. J Geochem Explor 100:97–104. doi:10.1016/j.gexplo.2008.08.002

Nordstrom DK, Blowes DW, Ptacek CJ (2015) Hydrogeochemistry and microbiology of mine drainage: an update. Appl Geochem 57:3–16. doi:10.1016/j.apgeochem.2015.02.008

Piper AM (1944) A graphic procedure in the geochemical interpretation of water-analyses. Trans Am Geophys Union 25. doi:10.1029/TR025i006p00914

Qureshi A, Maurice C, Öhlander B (2016) Potential of coal mine waste rock for generating acid mine drainage. J Geochem Explor 160:44–54. doi:10.1016/j.gexplo.2015.10.014

Schneider RL, Muhlmann H, Tommasi E, Medeiros RA, Daemon RA, Nogueira AA (1974) Revisão estratigráfica da Bacia do Paraná. Proceedings of XXVIII Congresso Brasileiro de Geologia, Porto Alegre, pp 41–65

SEMA (Secretaria de Estado do Meio Ambiente e Recursos Hídricos do Paraná) (2010) Bacias Hidrográficas do Paraná. SEMA, Curitiba

Shim MJ, Choi BY, Lee G, Hwang YH, Yang J, O'Loughlin EJ, Kwon MJ (2015) Water quality changes in acid mine drainage streams in Gangneung, Korea, 10 years after treatment with limestone. J Geochem Explor 159:234–242. doi:10.1016/j.gexplo.2015.09.015

Shuqair MSS (2002) Estudo da contaminação do solo e água subterrânea por elementos tóxicos originados dos rejeitos das minas de carvão de Figueira no Estado do Paraná. PhD Thesis, Universidade de São Paulo, São Paulo

Silva LFO, Wollenschlager M, Oliveira MLS (2011) A preliminary study of coal mining drainage and environmental health in the Santa Catarina region, Brazil. Environ Geochem Health 33:55–65. doi:10.1007/s10653-010-9322-x

Silva LFO, Vallejuelo SFO, Martinez-Arkarazo I, Castro K, Oliveira MLS, Sampaio CH, Brum IAS, Leão FB, Taffarel SR, Madariaga JM (2013) Study of environmental pollution and mineralogical characterization of sediment rivers from Brazilian coal mining acid drainage. Sci Total Environ 447:169–178. doi:10.1016/j.scitotenv.2012.12.013

Simate GS, Ndlovu S (2014) Acid mine drainage: challenges and opportunities. J Environ Chem Eng 2:1785–1803. doi:10.1016/j.jece.2014.07.021

Sun J, Tang C, Wu P, Strosnider WHJ, Han Z (2013) Hydrogeochemical characteristics of streams with and without acid mine drainage impacts: a paired catchment study in karst geology, SW China. J Hydrol 504:115–124. doi:10.1016/j.jhydrol.2013.09.029

USEPA (United States Environmental Protection Agency) (1994) Technical document acid mine drainage prediction. Washington, 48 p. http://water.epa.gov/polwaste/nps/upload/amd.pdf

Wolkersdorfer C (2008) Water management at abandoned flooded underground mines. Fundam Tracer Tests Model Water Treat. doi:10.1007/978-3-540-77331-3

Younger PL, Banwart SA, Hedin RS (2002) Mine water: hydrology, pollution, remediation. Kluwer Academic Publishers, Dordrecht. doi:10.1007/978-94-010-0610-1

Zacharias AA, Assine ML (2005) Modelo de preenchimento de vales incisos por associações de fáceis estuarinas, Formação Rio Bonito no Norte do Estado do Paraná. Rev Bras Geosci 35:573–583